

Machine Learning-based Classification of Active Walking Tasks in Older Adults using fNIRS

Dongning Ma, Meltem Izzetoglu, Roe Holtzer, and Xun Jiao

Abstract—Decline in gait features is common in older adults and an indicator of disability and mortality. Cortical control of gait, specifically in the pre-frontal cortex as measured by functional near infrared spectroscopy (fNIRS), during dual task walking has shown to be moderated by age, gender, cognitive status, and various age-related disease conditions. In this study, we develop classification models using machine learning methods to classify active walking tasks in older adults based on fNIRS signals into either Single-Task-Walk (STW) or Dual-Task-Walk (DTW) conditions. The fNIRS measurements included oxyhemoglobin (HbO₂) and deoxyhemoglobin (Hb) signals obtained from prefrontal cortex (PFC) of the subject performing on the ground active walking tasks with or without a secondary cognitive task. We extract the fNIRS-related features by calculating the minimum, maximum, mean, skewness and kurtosis values of Hb and HbO₂ signals. We then use feature encoding to map the values into binary space. Using these features, we apply and evaluate various machine learning methods including logistic regression (LR), decision tree (DT), support vector machine (SVM), k-nearest neighbors (kNN), multilayer perceptron (MLP), and Random Forest (RF). Results showed that the machine learning models can achieve around 97% classification accuracy.

Index Terms—functional near infrared spectroscopy, machine learning, aging, active walking

I. INTRODUCTION

Mobility impairments are common in healthy aging as well as age-related disease conditions such as mild cognitive impairments and dementia [1]–[7]. Limitations in walking, specifically decline in gait speed is associated with various adverse outcomes including higher rates of morbidity, loss of independence and mortality [8], [9]. Hence, impairments in locomotion can affect the individuals and their families detrimentally and pose a major public health challenge to society [9], [10].

Identifying mechanisms of mobility impairments is of vital importance in developing risk assessment and intervention procedures to ameliorate mobility decline and disability in aging populations. Motor control models of locomotion and robust associations between structural changes in frontal and subcortical brain regions with mobility outcomes have been established [11]–[13]. Even though converging evidence suggest the role cognitive processes, specifically the executive functions in explaining mobility performance and decline in older adults [14], [15], studies on the real time assessment of functional neural correlates of simple and attention-demanding locomotion tasks is scarce. This gap could be in part due to

the requirements of subject immobility and supine positioning in traditional neuroimaging modalities during scanning procedures making functional imaging of real, on the ground walking unattainable.

Recent studies began to increasingly utilize an emerging neuroimaging modality, namely functional near infrared spectroscopy (fNIRS) to assess cortical control and functional networks of mobility in aging populations [1]–[7], [16]–[25]. fNIRS is an optics based noninvasive, safe, portable, and wearable neuroimaging technique [26]–[30]. It can monitor relative changes in oxygenated-hemoglobin (HbO₂) and deoxygenated-hemoglobin (Hb) associated with cognitive activity using the light–tissue interaction properties of light within the near infrared range (650 – 950nm) [31]–[34]. fNIRS has been widely applied for the monitoring of functional activity in executive function, attention, memory, motor, visual, auditory and language domains and well validated against traditional neuroimaging methods [26]–[30]. Since it was less prone to movement artifacts and allow imaging of the brain functioning in upright and mobile conditions it is also well suited for the study of cognitive control of mobility in aging during active walking tasks [16]–[25].

While the tasks used in the investigation of functional brain mechanisms of mobility using fNIRS technology varies across studies, the most commonly implemented ones involve the walking under single- and dual-task conditions [1]–[7], [16]–[25]. The well validated dual-task walking (DTW) paradigm has been used to determine the effect of increased demands on attentional resources on gait performance which has emerged as a key risk factor for incident frailty, disability and mortality [35]. Specifically, in prior studies reproducible and statistically significant results have been found in HbO₂ values as measured by fNIRS from the PFC which increased in DTW as compared to STW due to greater cognitive demands that are inherent in the former walking condition [16]–[25]. Furthermore, it was found that cortical responses to task demands specifically in the DTW condition were moderated by age [17], gender and stress [18], fatigue level [19], medication use [21], and disease status including diabetes [22], Multiple Sclerosis (MS) [23], mild cognitive impairments [24], and neurological gait abnormalities [7].

Even though these growing number of studies that utilized fNIRS measures during DTW paradigms on older adults have repeatedly shown via statistical comparisons that hemodynamic biomarkers from PFC can discriminate between various walking task conditions and disease populations, their automatic classification using machine learning algorithms

have not yet been studied. Automatic detection of attention demanding vs simple walking tasks using discriminative hemodynamic features extracted from HbO₂ and Hb not only can provide information on an individual's use of his/her attentional resources but can also lead to diagnosis, monitoring and classification of different age-related disease conditions. fNIRS measures have been used in the classification of wide range of tasks and disease populations in different age groups before such as in applications for monitoring of mental workload, motor imagery, auditory and visual perception, various brain computer interfaces, pain assessment, anesthesia monitoring, attention deficit and hyperactivity disorder (ADHD) diagnosis, cognitive decline in traumatic brain injury, diagnosis of various mental illnesses such as schizophrenia [35]–[43]. There are a few studies on the classification of intentions for the initiation or stopping of walking, its step size and speed primarily for gait rehabilitation applications to control assistive devices such as prostheses or exoskeletons. Such studies primarily monitored motor areas and investigated classification of intentions or preparations to different types of gaits in healthy young adults where classification accuracy was found $\sim 80\%$ ranges [44]–[47]. In these small number of prior work, fNIRS measures from PFC during simple and attentionally demanding dual-task walking conditions that are indicative of different cognitive states and disease conditions in elderly populations were not studied with machine learning models and algorithms.

In this study our aim is to achieve automatic classification between active walking under simple (STW) and more cognitively taxing conditions (DTW) in older adults using fNIRS measures from the PFC with high accuracy. We have used our previously collected fNIRS data set from community residing healthy older adults ($n=451$) while they were performing STW and DTW tasks [6]. We have extracted features from HbO₂ and Hb signals such as maximum, minimum, mean, skewness and kurtosis, and used them with/without gender information and the Repeatable Battery for the Assessment of Neuropsychological Status (RBANS) outcome in various machine learning models to accurately classify the two walking activities. Among the evaluated machine learning algorithms including logistic regression (LR), support vector machine (SVM), k-nearest neighbors (kNN), multilayer perceptron (MLP) and random forest (RF), our findings indicated that LR generated the highest accuracy (97%) when fNIRS features together with gender and RBANS scores are used. To the best of our knowledge, we are the first to apply machine learning methods in fNIRS-based walking task classification in older adults achieving high accuracy.

This paper is organized as follows: In Section II, we introduce the information of the participants and our task protocol. In Section III, we explain our proposed methods in detail. We present the results of our comprehensive results in Section IV and finally, we provide concluding remarks and suggestions for future work in Section V.

II. PARTICIPANTS AND TASK PROTOCOL

A. Participants

The study involved a total of $n = 451$ community dwelling older adults in lower Westchester county, NY of age ≥ 65 years and older (76.16 ± 6.67 , 223 females) who were originally enrolled in a longitudinal cohort study entitled “Central Control of Mobility in Aging” (CCMA) [1], [6]. Recruitment procedures started with the identification of potential participants from population lists and then conducting a structured telephone interview to obtain verbal assent, assess medical history, mobility and cognitive functioning. Participants with significant loss of vision and/or hearing, inability to ambulate independently, current or history of severe neurological or psychiatric disorders, and recent or anticipated medical procedures that may affect mobility were excluded from the study. Individuals who agreed to participate in the study, fell into the inclusion/exclusion criteria and passed the phone interview were invited to two annual in-person study visits each lasting around three hours at the research center at Albert Einstein College of Medicine, Bronx, NY. During these visits, participants received a structured neurological examination and comprehensive neuropsychological, psychological, functional, and mobility assessments. Functional brain monitoring using fNIRS during the single- and dual-task walking protocol was completed in one session. Cognitive status was determined at consensus diagnostic case conferences [48]. RBANS was used to characterize overall level of cognitive function [49]. The sample was relatively healthy (Global Health Status mean score = 1.62 ± 1.09) and in the average range of overall cognitive function (RBANS mean Index score = 91.77 ± 11.71). The work described in this manuscript has been executed in adherence with The Code of Ethics of the World Medical Association (Declaration of Helsinki) and the APA ethical standards set for research involving human participants. Written informed consents were obtained at the first clinic visit according to study protocols approved by the Institutional Review Board at Albert Einstein College of Medicine, Bronx, NY.

B. Task Protocol

The task protocol used in this study involved two single tasks and one dual-task conditions presented in a counterbalanced order using a Latin-square design to minimize task order effects on the outcome measures. The single task conditions were 1) single-task walking (STW) and 2) the cognitive interference task (Alpha). In STW condition, participants were asked to walk at their “normal pace” around a 4×14 foot electronic walkway (Zenometrics system with Zeno electronic walkway using ProtoKinetics Movement Analysis Software (PKMAS), Zenometrics, LLC; Peekskill, NY). In the Alpha condition participants were asked to stand still on the electronic walkway while reciting alternate letters of the alphabet out loud (A, C, E...) for 30 seconds. In the dual-task walking (DTW) condition, participants were required to perform the two single tasks at the same time by walking around the walkway at their normal pace while reciting alternate letters of the alphabet. Participants were specifically asked to pay equal attention to both the walking and cognitive

interference tasks to minimize task prioritization effects. In both STW and DTW conditions participants were asked to walk on the instrumented walkway in three continuous loops that consisted of six straight walks and five left-sided turns. The duration of each task condition varied depending on the individual's walking speed. Reliability and validity for this walking paradigm have been well established [50].

III. METHODS

An overview of the proposed methods utilized in this work is illustrated in Fig. 1. We have four major steps: data collection, data pre-processing, feature extraction and applying machine learning models:

- **Data Collection:** In data collection, participants were asked to complete the task protocol as instructed, during which their hemodynamic activations were collected using fNIRS. In addition, we also collected subject-related data (gender and RBANS) of the participants.
- **Data Pre-processing:** In data pre-processing, we apply different methods such as visual inspection, wavelet denoising, hemodynamic data conversion, and spline and low pass filterings to obtain HbO₂ and Hb data of participants in time domain for different task conditions.
- **Feature Extraction:** We extract features by calculating the maximum, minimum, mean, kurtosis and skewness values of the Hb and HbO₂ signals in different task conditions. The value is calculated as an average of the left and right hemisphere of the brain, corresponding to channel 1-8 and channel 9-16. We then combined those hemodynamics fNIRS-related hemodynamics data with subject-related data of gender and RBANS scores to build up our features vectors to be used in machine learning models.
- **Applying Machine Learning:** We applied various machine learning algorithms in establishing machine learning models using *scikit-learn* framework [51]. We fine-tuned the model by considering different hyperparameters and configurations, and analyzed the trade-off between classification accuracy and computational efficiency.

A. Data Collection

fNIRS System We have utilized the fNIRS Imager 1100 (fNIRS Devices, LLC, Potomac, MD) in this study to collect the hemodynamic activations in the PFC while participants were performing the task protocol [6], [26], [27], [52]. In this fNIRS device, the sensor consists of 4 LED light sources and 10 photodetectors configured as shown in Fig. 2(a) where each source-detector separation is set to 2.5 cm. The light sources on the sensor (Epitex Inc. type L4X730/4X805/4X850-40Q96-I) contain three built-in LEDs having peak wavelengths at 730, 805, and 850 nm, with an overall outer diameter of 9.2 ± 0.2 mm. The photodetectors (Texas Instruments, Inc., type OPT101) are monolithic photodiodes with a single supply transimpedance amplifier. With the given source-detector configuration and the serial data collection regime of the device, hemodynamic changes in the PFC can be monitored at the sampling rate of 2 Hz with 16 voxels as shown in Fig. 2(b).

During the fNIRS data collection procedure, first the fNIRS sensor was placed on the forehead of the recruited participants. A standardized sensor placement procedure based on landmarks from the international 10–20 system was implemented [52], [53] where middle of the sensor was aligned with the nose horizontally and the bottom of the sensor was placed right above the eyebrows vertically. Testing was conducted in a quiet room. Participants wore comfortable footwear and performed the task protocol with the fNIRS sensor attached to their forehead during the overall data collection period.

B. Data Pre-processing

First, visual inspection was performed on individual data from all voxels to identify and eliminate the ones with saturation, dark current conditions or extreme noise. Then to eliminate spiky type noise, wavelet denoising with Daubechies 5 (db5) wavelet was applied to the raw intensity measurements at 730 and 850 nm wavelengths as proposed in [54] and widely applied in fNIRS studies [55]. The artifact-removed raw intensity measurements were then converted to changes in HbO₂ and Hb using modified Beer-Lambert law (MBLL) [25], [27], [34]. In MBLL, previously published values for conversion parameters i.e. wavelength and chromophore dependent molar extinction coefficients (ϵ) and age and wavelength adjusted differential pathlength factor (DPF) were used [25], [27], [56]. Finally, we applied Spline filtering [57] followed by a finite impulse response low-pass filter with cut-off frequency at 0.08 Hz [25], [58] to HbO₂ and Hb data separately to remove possible baseline shifts and to suppress physiological artifacts such as respiration and Mayer waves.

Data epochs corresponding to each task condition, STW, Alpha and DTW, were extracted to be used in further processing for feature extraction and machine learning model generation for automatic activity classification. fNIRS data acquisition and the electronic walkway system for gait analysis were synchronized using a central “hub” computer with E-Prime 2.0 software where time stamps of start and end points for each baseline and task condition were marked and recorded [16]–[25]. In order to correctly extract the data epochs during the exact walking task execution periods, a second level processing time synchronization method was implemented. The HbO₂ and Hb data epochs corresponding to time interval between the first recorded foot contact with the walkway until the end of the 6th and final straight walk algorithmically determined by PKMAS as previously described in [7] were extracted for STW and DTW conditions. Finally, proximal 10-second baselines administered prior to each experimental task were used to determine the relative task-related changes in the extracted HbO₂ and Hb data epochs for each of the task condition using the previously described baseline correction method (subtracting the average value of the proximal baseline region data from the following task epoch data) [16]–[25]. As our prior studies had suggested that DTW and STW are the most pronounced differentiating task conditions in aging and age-related diseases [6], [7], [16]–[25], we only used HbO₂ and Hb data epochs in DTW and STW tasks in further feature extraction and machine learning model development to automatically classify these two tasks in this work.

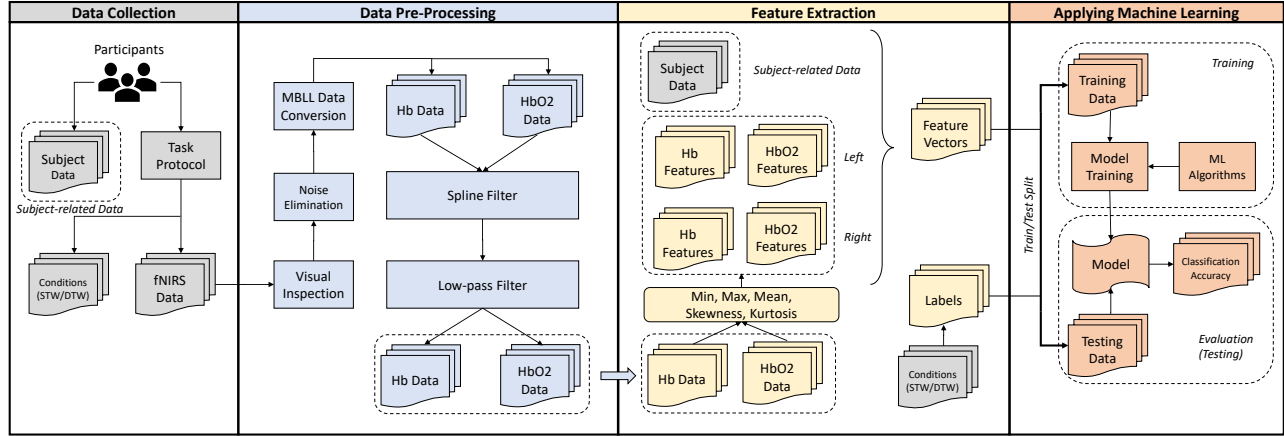


Fig. 1: Overview.

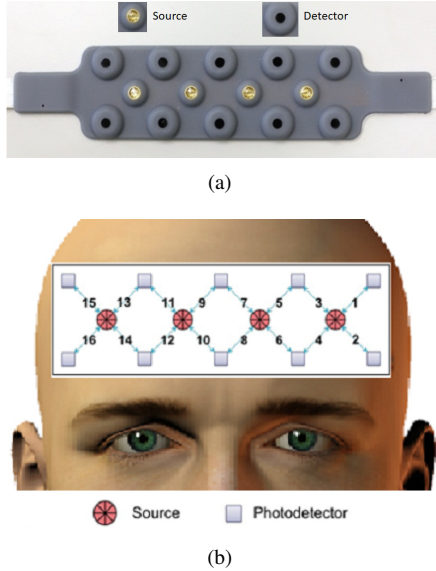


Fig. 2: fNIRS system (a) the sensor pad; (b) sensor placement on the forehead with 16 voxel locations.

C. Feature Extraction

fNIRS-related features fNIRS-related features used in this study were extracted from Hb and HbO₂ data in STW and DTW conditions. The data were in different time lengths for each walking task and subject because normal pace and hence task completion time differed between subjects and task conditions. For consistency, we select to use all of the time samples within the first 60 seconds of both Hb and HbO₂ data which corresponds to at most 120 samples of data since the sampling rate was 2Hz. For all the 16 channels in the fNIRS sensor pad, the total datapoints, namely the dimension of fNIRS-related features, is 16 (channels) * 120 (samples) * 2 (Hb and HbO₂) = 3840 at maximum, which is unrealistically high for machine learning. Therefore, to reduce dimensionality, we calculate the statistical values such as maximum, minimum, mean, skewness and kurtosis as the

features for each channel. We further split the 16 channels into left hemisphere (channel 1-8) and right hemisphere (channel 9-16) and calculate the average statistical values as the features for each hemisphere. Thus the dimension of fNIRS-related features are reduced to 2 (hemispheres) * 5 (statistical features) * 2 (Hb and HbO₂) = 20. This way issues such as different data lengths due to varying walking speeds across individuals and missing channel recordings due to noise elimination were also resolved.

In addition, we observe that fNIRS features drastically vary across different subjects: from Fig. ?? we can observe that, although HbO₂ generally has a higher average and maximum value than Hb, both of them shows a very similar normal distribution pattern. Such distribution indicates that the features we extract from fNIRS data is strongly subject-dependent, thus are not feasible to directly feed into machine learning model. Therefore, to eliminate biases from individual subjects, we further perform **feature encoding** within each of the subjects. For each subject, we first collect the 20 features from STW and DTW, respectively. Then we compare the features from STW and the features from DTW. The feature with a higher value is then set to 1 and the feature with a lower value is thus set to 0. Therefore by feature encoding, we map a 20-dimension, floating point array into a 20-dimension binarized array based on the inequity between the two task conditions.

Subject-related features In addition to the fNIRS-related features, we also considered other subject-related features such as the gender (G) and neuropsychological status (S) based on RBANS since they were found as moderators of DTW performance previously [18]. These features were added as parallel columns with the fNIRS-related features to provide enhancement in classification accuracy.

Feature Vector and Label In summary, we established feature vectors to be used in machine learning algorithms composed of different fNIRS-related features (maximum, minimum, mean, skewness and kurtosis on the left and right hemispheres) and subject-related features (G and S) as shown in Eq. 1. The corresponding features are described in detail in Table I. We have used various machine learning models on these multiple

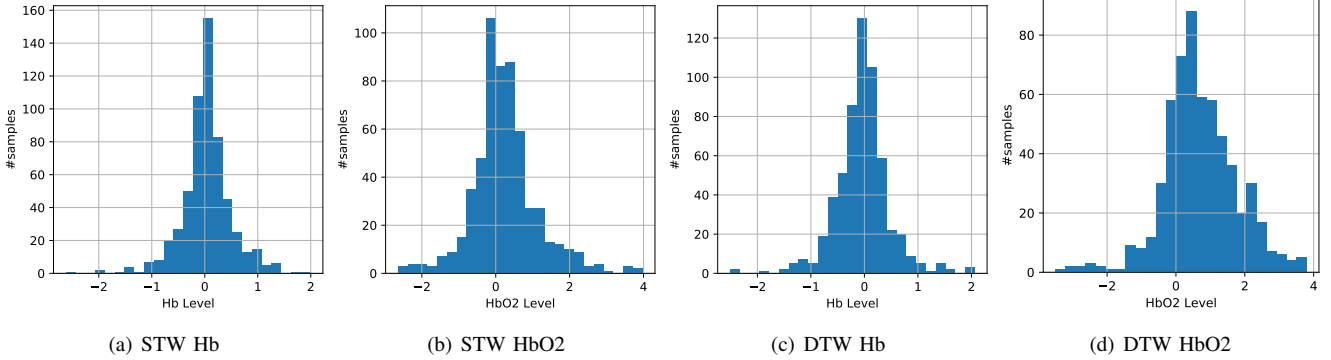


Fig. 3: Histogram of average Hb and HbO2 levels of different subjects under STW and DTW.

fNIRS- and subject-related feature combinations to evaluate their performance in the classification of STW and DTW conditions which will be discussed in Section IV. The labels were the corresponding task conditions (either STW or DTW) obtained from the task protocol during the data collection.

$$[G \ S \ \mathbf{HbL} \ \mathbf{HbR} \ \mathbf{HbO2L} \ \mathbf{HbO2R}] \quad (1)$$

D. Machine Learning

We applied multiple machine learning algorithms as listed in Table II. such as decision tree (DT), support vector machine (SVM), k-nearest neighbors (kNN), multilayer perceptron (MLP) and random forest (RF). We first used DT and kNN for their success and advantage in bioinformatics-related applications and fast training and classification time [59], [60]. DT classifier behaves like a flow chart with different layers, using each node with a criterion on certain attributes (features) on the input data to classify them into different classes. kNN classifies an input by checking its k nearest neighbors' class. In our case, if majority of the neighbors belongs to STW, then the input is classified as STW, otherwise as DTW. For kNN, we tried two different parameters for k: 5 and 10, to observe their classification accuracy accordingly. However, because biomedical related data could often be multi-modal and have high dimension, decision tree and kNN suffers from disadvantages such as overgrown decision trees and high variation in the nearest neighbours, which could significantly impair the model performance.

We further implemented the SVM classifier known for handling high dimension data especially in biomedical application of which the dimension can be high. SVM tries to find a (hyper-)plane to divide (classify) the input data into categories. However, a significant drawback of SVM is that it requires quite long time to train with large volume of data, resulting in cost-ineffectiveness. Recently, neural networks have been gaining growing attention on various types of classification tasks, therefore, we also tried the MLP classifier. A typical MLP consists of one input layer to take input features, one output layer for predicting classes and one or more hidden layers with specific number of nodes. Since network architecture has drastic impact on classification accuracy, we implemented

three structures of MLPs: two MLPs with one hidden layer of 10 and 50 nodes and one MLP with two hidden layers of 10 nodes each. The major drawback of MLP is the model size to achieve competitive accuracy: to gain high accuracy, in general, more sophisticated network structures or more nodes need to be used, inhibiting the training and inference efficiency.

As an ensemble classifier from decision trees, we further used RF for the classification task. An RF represents a “forest” of decision trees. Different decision trees inside the RF will give different predictions on the classes based on the input. Then RF will use majority vote from the classifications to finally decide the output class of this input. RF considers the relations between each input feature and could prevent the issues with a single DT to grow overly deep with large variance, yet RF requires higher computation complexity and more time to train than DT. We tested RF of different structures with 5, 10, and 25 trees.

We adopted *scikit-learn*, a python-based machine learning platform that support various types of machine learning algorithms as our machine learning framework [51]. The configuration and hyperparameters we used for these algorithms are shown in Table II. We randomly split the training data and testing data in a ratio of 80% to 20%. We used the training data to establish the model and then used the testing data to evaluate the model in terms of the classification accuracy under each configuration. During classification, we also record the time on classifying 1000 samples of each machine learning algorithm and configuration applied, to evaluate the computational cost. The machine learning experiments were executed on a computer configuration of Intel Xeon Silver 4110 1-core 2-thread CPU with 32GB memory.

IV. EXPERIMENTAL RESULTS

In this section, we present the experimental results on the machine learning model for the classification of active walking tasks in older adults. We evaluate the impact of different feature combinations as well as different machine learning algorithms on classification accuracy and computational efficiency.

TABLE I: Features used for machine learning. 5-dimension of fNIRS-related features include maximum, minimum, mean, skewness and kurtosis.

	Feature	Description	Dimension	Data Type
Subject-related	RBANS	Repeatable Battery for the Assessment of Neuropsychological Status	1	integer
	Gen	Gender (Male / Female)	1	binary
fNIRS-related	HbL	Features of Deoxygenated Hemoglobin from Left Hemisphere	5	binary
	HbR	Features of Deoxygenated Hemoglobin from Right Hemisphere	5	binary
	HbO2L	Features of Oxygenated Hemoglobin from Left Hemisphere	5	binary
	HbO2R	Features of Oxygenated Hemoglobin from Right Hemisphere	5	binary

TABLE II: Machine learning algorithms and their configuration

ML Algorithm	Configuration
logistic regression (LR)	
decision tree (DT)	n_trees = 5
random forest (RF)	n_trees = 10 n_trees = 25
support vector machine (SVM)	
k-nearest neighbors (kNN)	k = 5 k = 10
multilayer perceptron (MLP)	n_nodes = 10 n_nodes = 10, 10 n_nodes = 50

Parameters absent from this table are default from Scikit-learn.

A. Classification Accuracy Using Different Features

Features can impact machine learning model performance considerably. To understand the impact of different features, both fNIRS-related and subject-related, we conducted a comprehensive series of ablation experiments to examine the model performance in terms of accuracy using different feature combinations. Here, we chose to implement the model using logistic regression as the machine learning algorithm in all comparisons.

Table III shows the classification accuracy of different fNIRS-related feature combinations. With all the features included, the accuracy can achieve 96.68% at highest. First, by removing the features of maximum, minimum and mean values, the accuracy degrades to 80.74%, which indicates that those are critical features used by the machine learning algorithm. Next, by removing the kurtosis and skewness features from the overall feature set, the accuracy slightly drops to 95.9%. These two experiments reveal that although classification performance of using solely the kurtosis and skewness features is inferior, they can work with other features in synergy to improve the accuracy.

We also investigate the relative importance of Hb and HbO2. Using only Hb or HbO2 features, the accuracy drops to 97.56% and further to 95.9% or 95.51% when we remove the kurtosis and skewness features. Based on these experiments we observe that there is no significance on the importance of Hb or HbO2, and using both of the features achieves the highest accuracy.

B. Classification Accuracy Using Different Algorithms

In machine learning, in addition to the selected features, the types of algorithms and their configuration implemented in the analysis can also affect the model classification performance, tremendously. As introduced in Section III, to search for the best machine learning method and configuration for fNIRS-based active walking classification, we conducted a comprehensive series of experiments with various machine learning algorithms and configurations shown in Fig. II. We present the classification accuracy and the time consumed for classifying 1000 samples using different machine learning algorithms and configurations in Table IV.

We can observe that for all the examined algorithms, the classification accuracy is above 95%. Algorithms such as random forest (RFC), support vector machine (SVM), k-nearest neighbor (kNN) and Decision Tree produces mediocre accuracy from 95.9% to 97.54%. logistic regression (LR) and multilayer perceptron (MLP) with 10 or 50 hidden nodes achieve highest accuracy of 96.68%.

kNN (k=1) is the fastest amongst all the examined algorithms with less than 5 ms train time and 1.05 ms test time, however its accuracy of 95.9% is the lowest of all algorithms. Of the two most accurate algorithms, LR and MLP, LR is around 70X faster in training and 2X faster in testing than MLP. This is because neural networks like MLP have considerable amount of parameters to train and higher iterations for the model to obtain adequate accuracy.

C. Classification Accuracy Under Data Reduction

One major challenge of using machine learning in fNIRS-related applications is the ‘‘Small-N’’ problem. It means the samples, or the size of datasets available is extremely limited. To examine the performance of our model under limited dataset, we perform two types of experiments regarding dataset reduction.

First, we reduce the number of subjects used in training. Without dataset reduction, we have a total number of 451 subjects by default. We record the classification of the LR model using only 25%, 50% and 75% of them. We can observe from Fig. 4(a) that, using reduced size of training dataset will cause degradation in accuracy. Slight reduction in dataset size, e.g., from 100% to 75% does not impact the accuracy significantly. However, as the reduction grows, the accuracy degrades exponentially from around 97% to 73%.

Second, we reduce the time length of fNIRS-related signals used in the feature extraction. By default, we use 60 seconds

TABLE III: Ablation experiments: Classification accuracy with different features included.

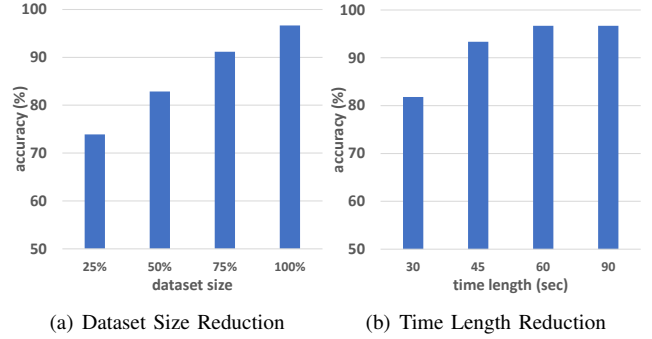
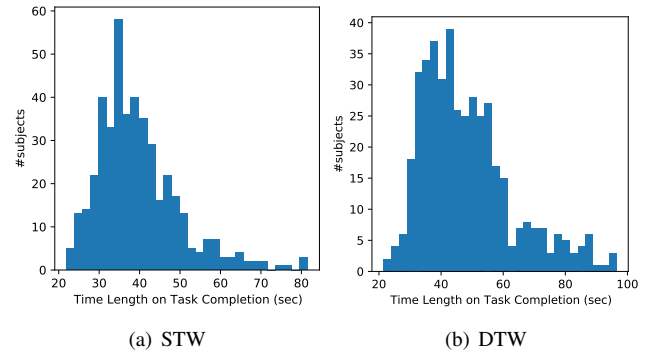
Hb					HbO2					Accuracy (%)
Max	Min	Mean	Kurtosis	Skewness	Max	Min	Mean	Kurtosis	Skewness	
X	X	X	X	X	X	X	X	X	X	96.68
			X	X				X	X	75.73
X	X	X			X	X	X			94.39
					X	X	X	X	X	96.13
X	X	X	X	X						96.13
					X	X	X			94.39
X	X	X								94.13

TABLE IV: Classification accuracy and time using different machine learning algorithms and configurations

Algorithm	Accuracy (%)	Train Time (ms)	Test Time (ms)
LR	96.68	7.4	1.1
DT	95.45	2.87	1.04
RFC_5	95.87	9.35	1.86
RFC_10	96.13	14.02	2.27
RFC_25	96.39	31.95	3.62
SVM	96.00	6.59	2.3
kNN_5	95.09	8.65	1.25
kNN_1	92.73	4.95	1.05
MLP_10	95.45	415.57	1.87
MLP_10, 10	96.00	595.48	1.99
MLP_50	96.13	627.94	2.1

of fNIRS signals to extract features for the machine learning model. According to the fNIRS experiments we acknowledge that while for most subjects, the time lengths to complete the task is around 30 – 40 seconds for STW and 35 – 50 seconds for DTW, it can significantly vary from 20 seconds to 100 seconds as shown in 5. Therefore, we evaluated the accuracy of the machine learning model when up to 30, 45, 60 and 90 seconds of data is considered as shown in Fig. 4(b). First we can observe that, the machine learning model performs inferior when using reduced time length of signals as the accuracy drops from around 97% to 81% when the time length is reduced from 60 seconds to 30 seconds. This outcome may suggest that the discriminative information within the select fNIRS features between the two task conditions can be diminished if shorter data segments are used. However, using longer time length does not always guarantee a higher accuracy. When using 90 seconds of fNIRS signal which is 30 seconds longer than the default 60 seconds, the accuracy does not gain additional increases. This finding could also be due to the fact that the number of participants having data length higher than 60 seconds were low to cause significant difference in the already very high accuracy values obtained when up to 60 seconds of data is used.

The counter-intuitive observation when using 90 seconds time length indicates useful features from the fNIRS signal may not expand throughout the entire time length, as increasing the time length included in the feature extract from 60 seconds to 90 seconds does not yield a higher accuracy in classification. From the dataset reduction experiments, the most useful feature may exist within around the first 60 seconds based on our observation.


Fig. 4: Classification accuracy under data reduction.

Fig. 5: Histogram of time lengths for task completion.

V. CONCLUSION

In this study, we have applied machine learning methods on extracted fNIRS-based hemodynamic features in together with gender and cognitive status information for the classification of walking tasks in older adults for the first time. We extracted useful feature representations such as maximum, minimum, mean kurtosis and skewness values, based on which we trained machine learning models using various algorithms including logistic regression, random forest and neural networks. We compare various feature combinations and different machine learning models and hyperparameter configurations in terms of their classification accuracy and computational efficiency to select the best model. Our machine learning model showed high performance on the classification of active walking tasks in older adults, with accuracy of around 97% using logistic regression over fNIRS-related features, combined with subject-related features of gender and RBANS. As we have shown here that automatic classification of active walking tasks in older

adults can be successfully achieved by using appropriate machine learning models and discriminative features, our future works involve classification of different age-related disease populations and healthy controls using the methods studied here.

REFERENCES

- [1] R. Holtzer, N. Epstein, J. R. Mahoney, M. Izzetoglu, and H. M. Blumen, "Neuroimaging of mobility in aging: A targeted review," *Journals of Gerontology Series A: Biomedical Sciences and Medical Sciences*, vol. 69, no. 11, pp. 1375–88, 2014.
- [2] R. Vitorio, S. Stuart, L. Rochester, L. Alcock, and A. Pantall, "Fmirs response during walking—artefact or cortical activity? a systematic review," *Neuroscience & Biobehavioral Reviews*, vol. 1, no. 83, pp. 160–72, 2017.
- [3] F. Herold, P. Wiegel, F. Scholkmann, A. Thiers, D. Hamacher, and L. Schega, "Functional near-infrared spectroscopy in movement science: A systematic review on cortical activity in postural and walking tasks," *Neurophotonics.*, vol. 4, p. 4, 2017.
- [4] D. Leff, F. Orihuela-Espina, C. E. Elwell, T. Athanasiou, D. T. Delpy, A. W. Darzi, and G. Z. Yang, "Assessment of the cerebral cortex during motor task behaviours in adults: A systematic review of functional near infrared spectroscopy (fmirs) studies," *Neuroim.*, vol. 54, no. 4, pp. 2922–36, 2011.
- [5] D. Hamacher, F. Herold, P. Wiegel, D. Hamacher, and L. Schega, "Brain activity during walking: A systematic review," *Neuroscience & Biobehavioral Reviews*, vol. 57, pp. 310–27, 2015.
- [6] R. Holtzer, J. R. Mahoney, M. Izzetoglu, C. Wang, S. England, and J. Verghese, "Online fronto-cortical control of simple and attention-demanding locomotion in humans," *Neuroimage.*, vol. 112, pp. 152–9, 2015.
- [7] R. Holtzer, J. Verghese, G. Allali, M. Izzetoglu, C. Wang, and J. R. Mahoney, "Neurological gait abnormalities moderate the functional brain signature of the posture first hypothesis," *Brain topo.*, vol. 29, no. 2, pp. 334–43, 2016.
- [8] M. Hirvensalo, T. Rantanen, and E. Heikkinen, "Mobility difficulties and physical activity as predictors of mortality and loss of independence in the community-living older population," *J Am. Geriatr. Soc.*, vol. 48, no. 5, pp. 493–498, 2000.
- [9] S. Studenski, S. Perera, K. Patel, C. Rosano, K. Faulkner, M. Inzitari, J. Brach, J. Chandler, P. Cawthon, E. B. Connor, M. Nevitt, M. Visser, S. Kritchevsky, S. Badinelli, T. Harris, A. B. Newman, J. Cauley, L. Ferrucci, and J. Guralnik, "Gait speed and survival in older adults," *JAMA*, vol. 305, no. 1, pp. 50–58, 2011.
- [10] J. Verghese, C. Wang, and R. Holtzer, "Relationship of clinic-based gait speed measurement to limitations in community-based activities in older adults," *Arch Phys Med Rehabil.*, vol. 92, pp. 844–846, 2011.
- [11] T. Drew, S. Prentice, and B. Schepens, "Cortical and brainstem control of locomotion," *Prog Brain Res*, vol. 143, pp. 251–261, 2004.
- [12] M. Lucas, M. E. Wagshul, M. Izzetoglu, and R. Holtzer, "Moderating effect of white matter integrity on brain activation during dual-task walking in older adults," *J Geront. Ser. A*, vol. 74, no. 4, pp. 435–441, 2019.
- [13] M. E. Wagshul, M. Lucas, K. Ye, M. Izzetoglu, and R. Holtzer, "Multi-modal neuroimaging of dual-task walking: Structural mri and fmirs analysis reveals prefrontal grey matter volume moderation of brain activation in older adults," *NeuroImage*, vol. 189, pp. 745–754, 2019.
- [14] R. Holtzer, C. Wang, and J. Verghese, "The relationship between attention and gait in aging: Facts and fallacies," *Motor Control*, vol. 16, pp. 64–80, 2012.
- [15] G. Yogev-Seligmann, J. M. Hausdorff, and N. Giladi, "The role of executive function and attention in gait," *Mov. Disord.*, vol. 23, no. 2, pp. 329–42, 2008.
- [16] R. Holtzer, M. Izzetoglu, M. Chen, and C. Wang, "Distinct fmirs-derived hbo2 trajectories during the course and over repeated walking trials under single-and dual-task conditions: Implications for within session learning and prefrontal cortex efficiency in older adults," *J. of Geront.: Ser. A*, 2018.
- [17] R. Holtzer, J. R. Mahoney, M. Izzetoglu, K. Izzetoglu, B. Onaral, and J. Verghese, "Fmirs study of walking and walking while talking in young and old individuals," in *J Geront, Ser. A: Biomed Sci. Med. Sci.* vol. 66, no. 8, 2011, pp. 879–87.
- [18] R. Holtzer, C. Schoen, E. Demetriou, J. R. Mahoney, M. Izzetoglu, C. Wang, and J. Verghese, "Stress and gender effects on prefrontal cortex oxygenation levels assessed during single and dual-task walking conditions," *European Journal of Neuroscience.*, vol. 45, no. 5, pp. 660–70, 2017.
- [19] R. Holtzer, J. Yuan, J. Verghese, J. R. Mahoney, M. Izzetoglu, and C. Wang, "Interactions of subjective and objective measures of fatigue defined in the context of brain control of locomotion," *The Journals of Gerontology: Series A.*, vol. 72, no. 3, pp. 417–23, 2017.
- [20] M. Chen, S. Pillemer, S. England, M. Izzetoglu, J. R. Mahoney, and R. Holtzer, "Neural correlates of obstacle negotiation in older adults: An fmirs study," *Gait & posture*, vol. 58, pp. 130–5, 2017.
- [21] C. J. George, J. Verghese, M. Izzetoglu, C. Wang, and R. Holtzer, "The effect of polypharmacy on prefrontal cortex activation during single and dual task walking in community dwelling older adults," *Pharmacological research*, vol. 139, pp. 113–9, 2019.
- [22] R. Holtzer, C. J. George, M. Izzetoglu, and C. Wang, "The effect of diabetes on prefrontal cortex activation patterns during active walking in older adults. brain and cognition," *vol.*, vol. 125, pp. 14–22, 2018.
- [23] M. E. Hernandez, R. Holtzer, G. Chaparro, K. Jean, J. M. Balto, B. M. Sandroff, M. Izzetoglu, and R. W. Motl, "Brain activation changes during locomotion in middle-aged to older adults with multiple sclerosis," *Journal of the neurological sciences*, vol. 370, pp. 277–83, 2016.
- [24] R. Holtzer and M. Izzetoglu, "Mild cognitive impairments attenuate prefrontal cortex activations during walking in older adults," *Brain Sci*, vol. 10, pp. 415–31, 2020.
- [25] M. Izzetoglu and R. Holtzer, "Effects of processing methods on fmirs signals assessed during active walking tasks in older adult," *IEEE Trans. on Neural Systems and Rehab. Eng.*, vol. 28, no. 3, pp. 699–709, 2020.
- [26] S. C. Bunce, M. Izzetoglu, K. Izzetoglu, B. Onaral, and K. Pourrezaei, "Functional near-infrared spectroscopy," *IEEE engineering in medicine and biology magazine*, vol. 25, no. 4, pp. 54–62, 2006.
- [27] M. Izzetoglu, K. Izzetoglu, S. Bunce, H. Ayaz, A. Devaraj, B. Onaral, and K. Pourrezaei, "Functional near-infrared neuroimaging," *IEEE Trans. on Neural Systems and Rehab. Eng.*, vol. 13, no. 2, pp. 153–9, 2005.
- [28] F. Scholkmann, S. Kleiser, A. J. Metz, R. Zimmermann, J. M. Pavia, U. Wolf, and M. Wolf, "A review on continuous wave functional near-infrared spectroscopy and imaging instrumentation and methodology," *Neuroimage.*, vol. 85, pp. 6–27, 2014.
- [29] S. Cutini, S. B. Moro, and S. Bisconti, "Functional near infrared optical imaging in cognitive neuroscience: An introductory review," *J. of Near Infrared Spectroscopy*, vol. 20, no. 1, pp. 75–92, 2012.
- [30] V. Quresima and M. Ferrari, "Functional near-infrared spectroscopy (fmirs) for assessing cerebral cortex function during human behavior in natural/social situations: A concise review," *Org. Res. Met.. 428116658959*, vol. 1094, 2016.

- [31] J. FF, "Noninvasive infrared monitoring of cerebral and myocardial oxygen sufficiency and circulatory parameters," *Science*, vol. 198, 1264–1267, 1977.
- [32] B. Chance, E. Anday, S. Nioka, *et al.*, "A novel method for fast imaging of brain function, non-invasively, with light," *Opt Express*, vol. 2, 411–423, 1998.
- [33] G. Strangman, D. A. Boas, and S. JP, "Non-invasive neuroimaging using near-infrared light," *Biol Psychiatry*, vol. 52, 679–693, 2002.
- [34] M. Cope and D. T. Delpy, "System for long-term measurement of cerebral blood and tissue oxygenation on newborn infants by near infra-red transillumination," *Med. Biol. Eng. Com.*, vol. 26, no. 3, 289–294, 1988.
- [35] F. Putze, S. Hesslinger, C.-Y. Tse, Y. Huang, C. Herff, C. Guan, and T. Schultz, "Hybrid fnirs-eeg based classification of auditory and visual perception processes," *Frontiers in neuroscience*, vol. 8, p. 373, 2014.
- [36] Y. Liu, H. Ayaz, and P. A. Shewokis, "Multisubject "learning" for mental workload classification using concurrent eeg, fnirs, and physiological measures," *Front. in Hum. Neurosci.*, vol. 11, p. 389, 2017.
- [37] A. M. Chiarelli, P. Croce, A. Merla, and F. Zappasodi, "Deep learning for hybrid eeg-fnirs brain-computer interface: Application to motor imagery classification," *J Neural Eng*, vol. 15, no. 3, p. 036028, 2018.
- [38] N. Naseer and K. S. Hong, "Fnirs-based brain-computer interfaces: A review," *Front. in Hum. Neurosci.*, vol. 9, p. 3, 2015.
- [39] A. Pourshoghi, I. Zakeri, and K. Pourrezaei, "Application of functional data analysis in classification and clustering of functional near-infrared spectroscopy signal in response to noxious stimuli," *J of Biomed. Optics*, vol. 21, no. 10, p. 101411, 2016.
- [40] G. Hernandez-Meza, M. Izzetoglu, M. Osbakken, M. Green, H. Abubakar, and K. Izzetoglu, "Investigation of optical neuro-monitoring technique for detection of maintenance and emergence states during general anesthesia," *J Clin. Monit. Comp.*, vol. 32, no. 1, pp. 147–163, 2018.
- [41] A. Guven, M. Altinkaynak, N. Dolu, M. Izzetoglu, F. Pektas, S. Ozmen, and T. Babat, "Combining functional near-infrared spectroscopy and eeg measurements for the diagnosis of attention-deficit hyperactivity disorder," *Neural Comp. Appl.*, vol. 3, pp. 1–4, 2019.
- [42] A. C. Merzagora, M. Izzetoglu, R. Polikar, V. Weisser, B. Onaral, and M. T. Schultheis, "Functional near-infrared spectroscopy and electroencephalography: A multimodal imaging approach," in *Int. Conf. on Found. of Aug. Cog.*, Berlin: Springer, 2019, pp. 417–426.
- [43] H. Song, L. Chen, R. Gao, I. I. Bogdan, J. Yang, S. Wang, W. Dong, W. Quan, W. Dang, and X. Yu, "Automatic schizophrenic discrimination on fnirs by using complex brain network analysis and svm," *BMC medical informatics and decision making*, vol. 17, no. 3, p. 166, 2017.
- [44] H. Jin, C. Li, and J. Xu, "Pilot study on gait classification using fnirs signals," *Comp. Intel. and Neurosci.*, 2018.
- [45] C. Li, J. Xu, Y. Zhu, S. Kuang, W. Qu, and L. Sun, "Detecting self-paced walking intention based on fnirs technology for the development of bci," *Medical & Biological Engineering & Computing*, vol. 21, pp. 1–9, 2020.
- [46] M. Rea, M. Rana, N. Lugato, P. Terekhin, L. Gizzi, D. Brötz, A. Fallgatter, N. Birbaumer, R. Sitaram, and A. Caria, "Lower limb movement preparation in chronic stroke: A pilot study toward an fnirs-bci for gait rehabilitation," *Neurorehabilitation and neural repair*, vol. 28, no. 6, pp. 564–75, 2014.
- [47] R. A. Khan, N. Naseer, N. K. Qureshi, F. M. Noori, H. Nazeer, and M. U. Khan, "Fnirs-based neurobotic interface for gait rehabilitation," *J Neuroeng. Rehab.*, vol. 15, no. 1, p. 7, 2018.
- [48] R. Holtzer, J. Verghese, C. Wang, C. B. Hall, and R. B. Lipton, "Within-person across-neuropsychological test variability and incident dementia," *JAMA*, vol. 300, no. 7, pp. 823–830, 2008.
- [49] K. Duff, J. D. H. Clark, S. E. O'Bryant, J. W. Mold, R. B. Schiffer, and P. B. Sutker, "Utility of the rbans in detecting cognitive impairment associated with alzheimer's disease: Sensitivity, specificity, and positive and negative predictive powers," *Archives of clinical neuropsychology : the official journal of the National Academy of Neuropsychologists*, vol. 23, pp. 603–612, 2008.
- [50] R. Holtzer, C. Wang, and J. Verghese, "Performance variance on walking while talking tasks: Theory, findings, and clinical implications," *Age (Dordr)*, vol. 36, no. 1, pp. 373–381, 2014.
- [51] F. Pedregosa, G. Varoquaux, A. Gramfort, V. Michel, B. Thirion, O. Grisel, M. Blondel, P. Prettenhofer, R. Weiss, V. Dubourg, *et al.*, "Scikit-learn: Machine learning in python," *The Journal of machine Learning research*, vol. 12, pp. 2825–2830, 2011.
- [52] H. Ayaz, P. A. Shewokis, A. Curtin, M. Izzetoglu, K. Izzetoglu, and B. Onaral, "Using mazesuite and functional near infrared spectroscopy to study learning in spatial navigation," *JoVE (Journal of Visualized Experiments)*, vol. 8, no. 56, e3443, 2011.
- [53] H. Ayaz, M. Izzetoglu, and S. M. Platek, "Registering fnir data to brain surface image using mri templates," in *Conf Proc IEEE Eng Med Biol Soc*, 2006, pp. 2671–4.
- [54] B. Molavi and G. A. Dumont, "Wavelet-based motion artifact removal for functional near-infrared spectroscopy," *Phys. Meas.*, vol. 33, no. 2, pp. 259–70, 2012.
- [55] A. M. Chiarelli, E. L. Maclin, M. Fabiani, and G. Gratton, "A kurtosis-based wavelet algorithm for motion artifact correction of fnirs data," *Neuroimage*, vol. 112, pp. 128–137, 2015.
- [56] F. Scholkmann and M. Wolf, "General equation for the differential pathlength factor of the frontal human head depending on wavelength and age," *Journal of biomedical optics*, vol. 18, no. 10, p. 5004, 2013.
- [57] F. Scholkmann, S. Spichtig, T. Muehlemann, and M. Wolf, "How to detect and reduce movement artifacts in near-infrared imaging using moving standard deviation and spline interpolation," *Physiological measurement*, vol. 31, no. 5, p. 649, 2010.
- [58] M. A. Yücel, S. J., C. M. Aasted, P. Y. Lin, D. Borsook, L. Becerra, and D. A. Boas, "Mayer waves reduce the accuracy of estimated hemodynamic response functions in functional near-infrared spectroscopy," *Biomedical optics express*, vol. 7, no. 8, pp. 3078–3088, 2016.
- [59] D. Che, Q. Liu, K. Rasheed, and X. Tao, "Decision tree and ensemble learning algorithms with their applications in bioinformatics," in *Software tools and algorithms for biological systems*, Springer, 2011, pp. 191–199.
- [60] T. Prasartvit, A. Banharnsakun, B. Kaewkamnerdpong, and T. Achalakul, "Reducing bioinformatics data dimension with abc-knn," *Neurocomputing*, vol. 116, pp. 367–381, 2013.